

* This manuscript was accepted for publication in Advances in Space Research. Copyright 2010 Committee on Space Research. Further reproduction or electronic distribution is not permitted.

* For more information, please visit the author's webpage <http://www.jwseo.com>.

Correlation of GPS signal fades due to ionospheric scintillation for aviation applications

Jiwon Seo^a, Todd Walter, Per Enge

*Department of Aeronautics and Astronautics, Stanford University, 496 Lomita Mall,
Stanford, CA 94305, U.S.A.*

^a Corresponding author, jwseo@cs.stanford.edu

Abstract

Deep and frequent Global Positioning System (GPS) signal fading due to strong ionospheric scintillation is a major concern for GPS-guided aviation in equatorial areas during high solar activity. A GPS aviation receiver may lose carrier tracking lock under deep fading, and a lost channel cannot be used for position calculation until lock is reestablished. Hence, frequent loss of lock due to frequent fading can significantly reduce the availability of GPS aviation. However, the geometric diversity of the satellites can mitigate scintillation impact on GPS aviation depending on the correlation level of deep fades between satellites. This paper proposes a metric to measure the correlation level of two fading channels from the perspective of GPS aviation. Using this metric, the satellite-to-satellite correlation is studied based on real scintillation data. The low satellite-to-satellite correlation shown in this paper envisions notable availability benefit from the geometric diversity of satellites under strong scintillation. In addition, this paper proposes a way to generate correlated fading processes with arbitrary correlation coefficients. Using this correlated fading process model, the availability of Localizer Performance with Vertical guidance (LPV)-200 under severe scintillation scenarios is analyzed. The result emphasizes the importance of a fast reacquisition capability of an

aviation receiver after a brief outage, which is not currently mandated by the aviation receiver performance standards.

Keywords: Correlation; Ionospheric Scintillation; Global Positioning System (GPS); Wide Area Augmentation System (WAAS); Aviation; Availability

1. Introduction

The Global Positioning System (GPS) (Parkinson, 1997) with integrity information from the Wide Area Augmentation System (WAAS) (Enge et al., 1996) is currently used in the United States to guide the approach of aircraft down to 200 ft above the runway. This approach procedure, also known as Localizer Performance with Vertical guidance (LPV)-200 (Cabler and DeCleene, 2002), can be expanded globally by future Global Navigation Satellite Systems (GNSS) that provide dual frequency civilian codes in the aviation band (e.g., L1 and L5 frequencies) (Walter et al., 2008; Hegarty and Chatre, 2008). The ionospheric delay can be directly measured by future dual frequency GPS avionics, and higher-order ionosphere errors are not problematic for LPV-200 (Datta-Barua et al., 2008). However, deep and frequent GPS signal fades due to ionospheric scintillation (Crane, 1977; Gwal et al., 2004) raise a concern about the operational availability of LPV-200 in the equatorial area during solar maxima.

Deep and frequent signal fading, as observed during the past solar maximum (2001), can lead to frequent loss of the carrier tracking lock of GPS receivers. Even during low solar activity periods, there is a probability of losses of lock of multiple satellites, particularly during equinoctial months (Rama Rao et al., 2006). The loss of these satellites can significantly reduce navigation availability. However, the geometric diversity of GPS satellites can mitigate the impact of scintillation on GPS aviation. A GPS receiver may briefly lose a few satellites simultaneously, but if the receiver can track a minimum of four satellites with good geometry, GPS navigation is still possible (Misra and Enge, 2006; Kaplan and Hegarty, 2006). Hence, it is important to know the probability of

simultaneous loss of multiple satellites under strong scintillation for assessing mitigation effectiveness from the geometric diversity.

The conventional correlation coefficient between two time series of signal intensity shows the similarity of the trends of the two time series, but it does not describe how often both channels are lost simultaneously (Section 2). Hence, it is not a good metric for assessing scintillation impact on GPS aviation. Since there is no appropriate metric to measure the probability of simultaneous loss of satellites for aviation applications, this paper suggests a new correlation coefficient from the perspective of GPS aviation. This new correlation coefficient is proposed in Section 2 and mathematically justified in Section 4.

Using this improved correlation coefficient, the correlation of signal fades between different satellites is evaluated based on real scintillation data (Section 3). Further, the correlation of loss of lock between different satellites is also evaluated depending on a receiver's reacquisition time. (The difference between the correlation of deep fades and the correlation of loss of lock is explained in Section 3.) To the authors' knowledge, the satellite-to-satellite correlation of deep fades (and loss of lock) under strong scintillation has not been previously evaluated for the short time scales of receiver tracking loop closure.

The probability of simultaneous loss of two satellites can be explained by the correlation coefficient of loss of lock between the satellites. However, further analysis is required to obtain the operational availability of LPV-200 under correlated fading environments. A method to simulate correlated fading channels is proposed in Section 4. This method enables generating correlated fading processes with an arbitrary fading rate (number of deep fades per unit time) and an arbitrary correlation coefficient between satellites. Using this method, the availability of LPV-200 under severe scintillation scenarios is analyzed in Section 5. The sensitivity analysis of the availability is also performed with various correlation levels and various reacquisition times of a receiver.

2. Deep GPS signal fades and correlation coefficients

Electron density irregularities in the ionosphere can cause amplitude fading and phase jitter of transionospheric radio waves, which is referred to as ionospheric scintillation (Aarons, 1982; Jin et al., 2008). Most of the Carrier-to-Noise-density ratio (C/N_0) fluctuations due to scintillation in Fig. 1 (bottom) are not problematic for GPS aviation as the receiver is able to maintain its tracking lock. However, the deep signal fades (marked in red) causing loss of carrier tracking lock of a receiver are of real concern. The GPS aviation researchers' primary interest is not how a signal fluctuates, but whether a receiver loses lock due to deep fading.

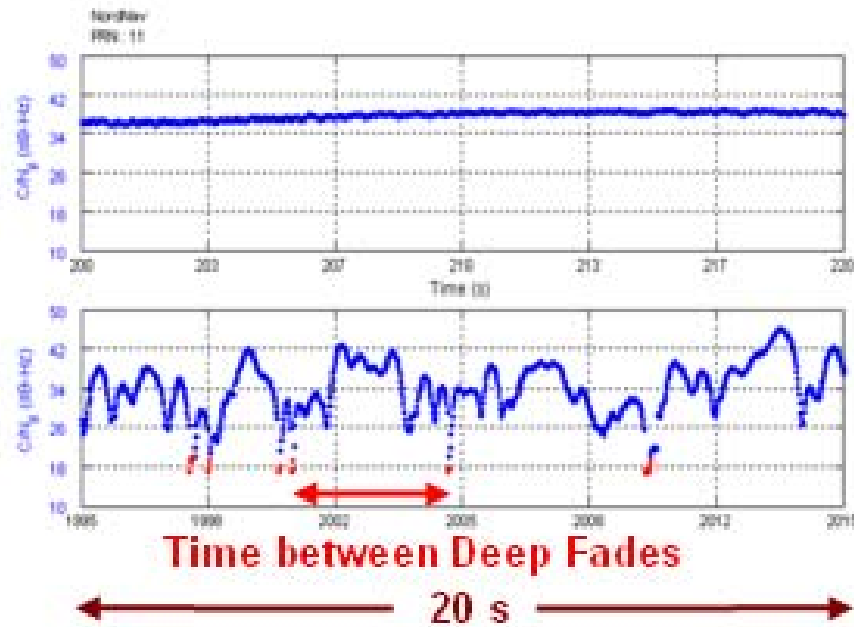


Fig. 1. Comparison of 50 Hz C/N_0 outputs of nominal (top) and scintillation (bottom) cases. This is a 20 s example from the data collected at Ascension Island in 2001. Samples from deep fades (20 dB-Hz or below) are marked in red.

As mentioned in Section 1, the geometric diversity of GPS satellites can mitigate the impact of scintillation. Although a receiver may lose a few satellites simultaneously, it can still provide position solutions if it tracks at least four satellites with good geometry. Hence, the correlation of deep fades between satellites should be well understood to

assess possible mitigation of the scintillation impact on GPS aviation. A high correlation of deep fades in this paper means that the deep fades of different satellite channels occur simultaneously with a high probability. This interpretation of correlation is exactly what interests GPS aviation researchers. However, the conventional definition of the sample correlation coefficient of Eq. (1) does not provide any information with respect to how often two channels fade simultaneously.

$$\hat{\rho} = \frac{\sum_i (x_i - \bar{x})(y_i - \bar{y})}{\sqrt{\sum_i (x_i - \bar{x})^2} \sqrt{\sum_i (y_i - \bar{y})^2}} \quad (1)$$

Fig. 2 illustrates a weakness of this definition of a sample correlation coefficient. The x_i and y_i of Eq. (1) are the C/N₀ sample points in green and blue in Fig. 2. The \bar{x} and \bar{y} are the mean values. In the top plot of Fig. 2, only one C/N₀ time series (blue) experiences deep fading. Hence, the receiver would still be able to track the other channel (green) although one channel (blue) is lost for a brief period of time after deep fading. The bottom plot of Fig. 2 represents a more challenging scenario. In this case, two channels sometimes fade simultaneously (red circles); as a result, the receiver loses two channels together during these outages.

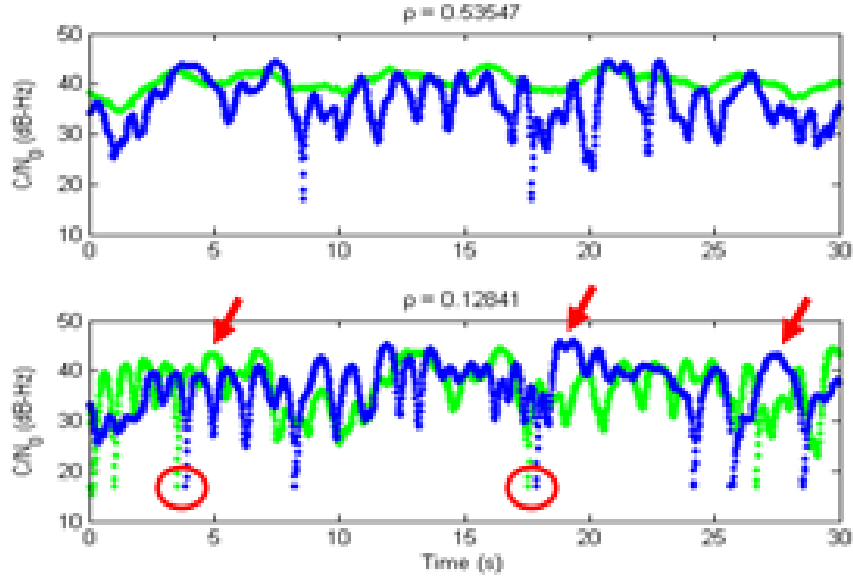


Fig. 2. Weakness of the conventional sample correlation coefficient. The bottom plot with simultaneous deep fades (red circles) is more problematic for GPS aviation than the top plot. However, the bottom plot has a lower correlation coefficient because of the opposite trends of the two C/N_0 time series (red arrows).

Obviously, the bottom plot represents a worse scenario for GPS navigation, but it has a lower sample correlation coefficient (0.13) than the other case (0.54) when the correlation coefficient of Eq. (1) is applied. In other words, the definition of Eq. (1) merely evaluates the similarity of the trends of two time series. The green series of Fig. 2 (top) follows the general trend of the blue series. Consequently, the correlation coefficient of the top figure is high. However, the green series of Fig. 2 (bottom) sometimes goes up while the blue series goes down and vice versa (red arrows), which significantly reduces its sample correlation coefficient. Again, GPS aviation researchers are interested in how often deep fades of different channels occur simultaneously. Deep fades are very brief and C/N_0 sample points during deep fades are few in number. Therefore, the sample points during deep fades have little influence on the sample correlation coefficient obtained by Eq. (1), which is dominated by the large number of sample points out of deep fades, which are not of primary interest.

Fig. 2 clearly demonstrates the weakness of the conventional definition of sample correlation coefficient for the study of scintillation impact on GPS aviation. We suggest

an alternative definition of a sample correlation coefficient as Eq. (2). (T is an observation time window.)

$$\hat{\rho}(T) = \frac{\text{Number of simultaneous deep fades between channel 1 and 2}}{\sqrt{\text{Number of deep fades of channel 1}}\sqrt{\text{Number of deep fades of channel 2}}} \quad (2)$$

The sample correlation coefficient of Eq. (2) exactly describes how often both channels fade simultaneously, by definition. This correlation coefficient varies between 0 and 1. The mathematical background of this correlation coefficient will be discussed in Section 4. The correlation study of this paper follows this definition of correlation coefficient.

3. Satellite-to-Satellite correlation under strong scintillation

3.1. Satellite-to-Satellite correlation during a past solar maximum period

As Conker et al. (2003) mentioned, a realistic estimate of the probability of simultaneous loss of multiple satellites is needed for evaluating scintillation impact on GPS aviation. A quantitative study about the probability of simultaneous loss of satellites is possible using the correlation coefficient proposed in Section 2. If the sample correlation coefficient of Eq. (2) is applied to study satellite-to-satellite correlation of deep fades, it can be interpreted as Eq. (3). (T is an observation time window.)

$$\hat{\rho}(T) = \frac{\text{Number of simultaneous deep fades between satellite 1 and 2}}{\sqrt{\text{Number of deep fades of satellite 1}}\sqrt{\text{Number of deep fades of satellite 2}}} \quad (3)$$

Following this interpretation, the sample correlation coefficients during the most severe scintillation periods of a campaign at Ascension Island are shown in Fig. 3.

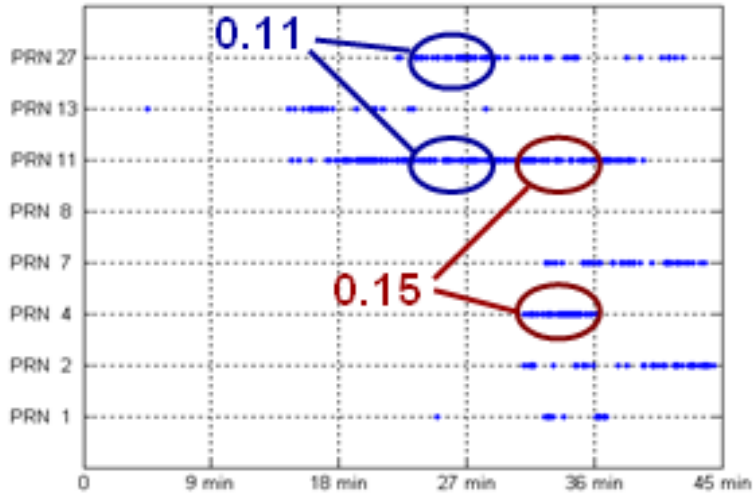


Fig. 3. Correlation of deep fades between two satellite channels under strong scintillation of the previous solar maximum. (The observation time window, T , is 300 s.) The blue points represent the instances of deep fades at the corresponding satellite channels. Seven satellites were fading during the worst 45 min scintillation at Ascension Island, but the maximum correlation coefficient during the worst 300 s (in ellipses) was only 0.15, which was between PRN 4 and PRN 11.

The scintillation data were collected at Ascension Island for nine days during the past solar maximum (nine days between 13 March 2001 and 26 March 2001). The collected L1 data from a NAVSYS DSR-100 receiver (May et al., 1999) are in the format of raw Intermediate Frequency (IF) data. The raw IF data were postprocessed using a NordNav commercial software receiver (Normark and Stahlberg, 2005). The NordNav postprocessing was set up to enable immediate reacquisition after a brief outage for this data set. This paper defines a “deep fading” as a signal fading with a minimum C/N_0 of 20 dB-Hz or less in this particular data set. Based on our observations during a 36 day campaign in Brazil (E. R. de Paula et al., presented at SBAS-IONO Meeting, Boston, MA, June 15, 2007), a certified WAAS receiver tracked signal down to 28-30 dB-Hz. Due to the early IF capture technology of DSR-100 incorporating one-bit sampling, narrow bandwidth, and aliasing caused by a low sampling frequency, the C/N_0 level of the Ascension Island data is 8-10 dB lower than the typical C/N_0 level from a current IF recorder such as NordNav IF recorder. After adjusting this 8-10 dB difference caused by an early and a current receiver technology, the 20 dB-Hz threshold in the Ascension

Island data (2001) is comparable to 28-30 dB-Hz threshold of the certified aviation receiver in the Brazil campaign (2007).

Among the nine day data from Ascension Island, the worst 45 min scintillation was selected for Fig. 3. The worst 45 min period was selected based on S_4 indices and the number of satellites experiencing deep fades. During the worst 45 min, seven satellites out of eight experienced frequent deep fades, which implies that electron density irregularities covered almost all portions of the sky. (Their S_4 indices were over 1.2.) However, the worst-case correlation coefficient between PRN 4 and PRN 11 was only 0.15 during the worst 300 s and the worst-case correlation coefficient between PRN 11 and PRN 27 was only 0.11. Therefore, although seven satellites were affected by scintillation, the correlation of deep fades between different satellites was very low, which means that the probability of the simultaneous deep fades of multiple satellites was very low.

Note that this worst 45 min scintillation with seven affected satellites is not a common observation even in the equatorial area during solar maxima. For example, El-Arini et al. (2003) reported maximum of four satellites under scintillation during the campaign in Naha, Japan, which is also located in the equatorial anomaly region where strong scintillation is highly expected. In addition to the intensity of scintillation, the number of satellites affected by scintillation is also a very important factor for GPS aviation, because a minimum of four simultaneously tracked satellites with a good geometry is required for aviation. Hence, seven satellites under lower scintillation intensity, for example, may be more problematic for GPS aviation than three satellites with much higher scintillation intensity.

We have shown that the correlation of deep signal fades was very low even though almost all satellite channels experienced deep fading. However, the “correlation of loss of lock” of a receiver is not exactly the same as the “correlation of deep fades.” Even under the same signal environment, the correlation of loss of lock can be very different depending on a receiver’s reacquisition capability. For example, if deep fades of two

satellite channels are 2 s apart, a receiver does not experience an overlapping loss of lock if it can reestablish tracking the lost channel within 2 s. If it takes longer than 2 s, the receiver experiences overlapping loss of two satellites. Therefore, the recovery time of the lost channel after the reintroduction of signal, which is called “reacquisition time” in WAAS Minimum Operational Performance Standards (MOPS) (RTCA, 2006), should also be considered to properly measure the correlation of loss of lock of a receiver. When the sample correlation coefficient of Eq. (2) is applied to study satellite-to-satellite correlation of loss of lock, it can be interpreted as Eq. (4).

$$\hat{\rho}(T) = \frac{\text{Number of overlapping losses of lock between satellite 1 and 2}}{\sqrt{\text{Number of losses of lock of satellite 1}} \sqrt{\text{Number of losses of lock of satellite 2}}} \quad (4)$$

If a receiver’s reacquisition time is t , the loss of lock of satellite channel 1 and 2 within t results in an overlapping loss. With this interpretation, the sample correlation coefficients of loss of lock between two satellite channels are obtained in Table 1. As expected, longer reacquisition times result in higher correlation coefficients of loss of lock.

Table 1. Correlation coefficients of loss of lock between two satellite channels during the worst 300 s at Ascension Island depending on a receiver’s reacquisition time.

Satellite Pair	Reacquisition Time				
	1 s	2 s	3 s	4 s	5 s
PRN 4 & 11	0.18	0.30	0.34	0.38	0.45
PRN 11 & 27	0.18	0.38	0.47	0.53	0.57

The difference between the correlation coefficients of deep fades (Fig. 3) and the correlation coefficients of loss of lock (Table 1) should be emphasized. The correlation coefficient of deep fades in Fig. 3 describes the correlation level of “signal environment” between two satellite channels. The signal environment itself is independent of a receiver’s algorithm and performance. Hence, the reacquisition capability of a receiver was not considered to calculate the correlation coefficients in Fig. 3. The correlation coefficient of deep fades is estimated by assuming that the fades of different satellites are “simultaneous” if they are within a 0.5 s range. This is believed to be a conservative

estimation because the fading duration at 20 dB-Hz is about 0.2 s (95%) based on the fading duration model in Fig. 10 of (Seo et al., 2009). El-Arini et al. (2003) also observed about 0.2 s fading duration at 20 dB fading. If signal fades within 0.2 s are considered to be “simultaneous,” the sample correlation coefficients would be even lower than the coefficients in Fig. 3.

On the other hand, the correlation coefficient of loss of lock in Table 1 is affected by a receiver’s reacquisition capability on top of the correlation of signal environment. Consequently, it better describes the effective correlation of satellite channels experienced by a receiver. However, the correlation level of signal environment itself in Fig. 3 is also valuable information for the availability study in Section 5. Since the study requires generating correlated fading environment before considering a receiver’s reacquisition capability, we need to know the correlation level of signal environment itself. The details will be discussed in Section 5.

3.2. Correlation of closely-spaced satellites during a strong scintillation period of solar minimum

Electron density irregularities can cover large portions of the sky during solar maxima, but GPS signals from different satellites pass through different irregularities to a receiver. Hence, there is no strong physical reason to expect high probability of simultaneous fades between different satellite channels unless two satellites are located very close to each other. In fact, some GPS satellites (e.g., on-orbit spares) are located close to each other in the same orbital plane. The Ascension Island data set does not have scintillation of closely-spaced satellites, but we observed scintillation of closely-spaced satellites during a Brazil campaign (E. R. de Paula et al., presented at SBAS-IONO Meeting, Boston, MA, June 15, 2007). The Brazil data were collected at Sao Jose dos Campos for 36 days (December 2005 – January 2006) during solar minimum using a certified WAAS receiver. Although it was a solar minimum period, strong scintillation with a scintillation index (S_4 index) of about 1.0 was observed on the worst scintillation day (25 December 2005).

Red dots in Fig. 4 show the locations of loss of satellites during 5 hours (18:00 – 23:00, local time) on 25 December 2005. A certified aviation receiver is at the center of Fig. 4. The outer circle represents 6 degree elevation and the center point represents 90 degree elevation. The receiver lost carrier tracking lock on low elevation satellites, but loss of low elevation satellites is normal. (The low elevation here means an elevation below 5 degree mask angle.) Scintillation caused loss of higher elevation satellites (PRN 26, PRN 29) as well. These two closely-spaced satellites passed through the northern part of the sky at the same time and experienced loss of lock in the same time-frame for about an hour (22:00 – 23:00, local time). Hence, we can imagine that electron density irregularities were developed on the northern part of the sky during this period. Since the lock status of each satellite channel of the certified aviation receiver is known, the sample correlation coefficient of loss of lock between two satellite channels can be obtained by Eq. (4).

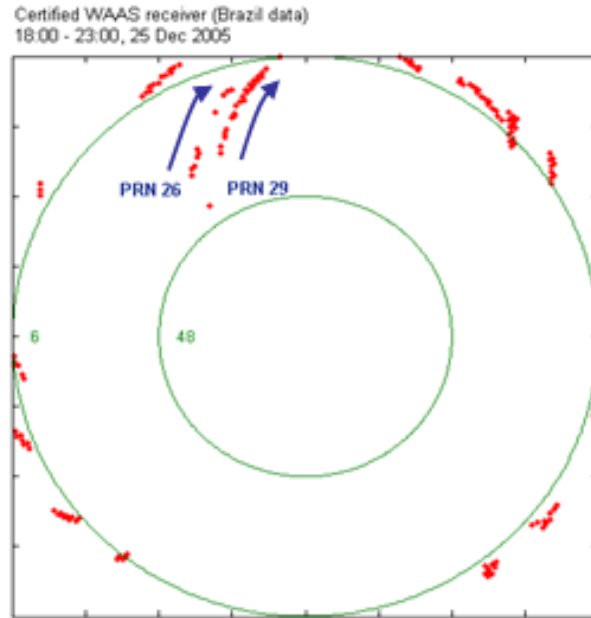


Fig. 4. Locations of loss of satellites (red dots) during 5 hours on 25 December 2005 at Sao Jose dos Campos, Brazil. Two closely-spaced satellites (PRN 26 and PRN 29) experienced loss of lock for about an hour, but there was no case of simultaneous loss of these two satellites. The data were collected by a stationary aviation receiver located at the center of this figure. The green lines represent elevation angle contours.

These Brazil data were collected at 1 Hz rate and the lock status of the certified receiver was also reported at every second. Interestingly enough, there was not even a single case of simultaneous loss of these two closely-spaced satellites during this one hour period of strong scintillation. Therefore, the sample correlation coefficient obtained by Eq. (4) is zero during this period. This is mainly because the certified receiver was capable of reacquiring lost channels quickly. Although the WAAS MOPS mandates up to 20 s reacquisition time (RTCA, 2006), the certified receiver reacquired lost channels within 2 s in 91% cases during this 36 day campaign (Seo et al., 2010).

Note that the zero correlation of loss of lock during this period is obtained from the actual response of the certified aviation receiver. If we assumed that the receiver would always take 4 s to reacquire the lost channels, for example, the correlation coefficient during this worst one hour could have been 0.06 which still demonstrates low correlation. The correlation coefficient could be higher if the ionospheric pierce points of the satellites were moving along the same magnetic meridian because of the field-aligned nature of the irregularities causing scintillation at low latitudes. However, the likelihood of this worst-case movement of multiple satellites is expected to be low. Hence, closely-spaced satellites do not necessarily result in a high probability of simultaneous loss as shown in this section, especially when a receiver's reacquisition time is much shorter than the 20 s requirement in the current WAAS MOPS.

We report very low correlation between closely-spaced satellites on the worst scintillation day of the 36 day campaign in Brazil. However, the Brazil data were collected during solar minimum, so the data do not contain the very frequent deep fades as observed during the past solar maximum. Therefore, the correlation between closely-spaced satellites under very frequent deep fades of solar maxima can be much higher than our observation, which should be carefully studied with extensive data during the next solar maximum (around 2013).

4. A method to generate correlated fading processes

This section proposes a method to simulate correlated fading channels with an arbitrary correlation coefficient between two channels. With this correlated fading process model and the observed correlation coefficients in Section 3, the availability of LPV-200 under severe scintillation scenarios will be evaluated in Section 5. Furthermore, this section provides a mathematical justification of the proposed correlation coefficient in Section 2.

In order to develop a method to generate correlated fading processes, we first studied the statistics of the time between deep fades during the worst 45 min scintillation at Ascension Island. (The definition of time between deep fades is given in Fig. 1.) The empirical Probability Density Function (PDF) of the time between deep fades during the worst 45 min is shown in Fig. 5. An interesting observation is that the distribution of time between deep fades during the worst 45 min approximately follows an exponential distribution. This data set contains very frequent deep fades. Seo et al. (2009) reported 5 s median time between deep fades during this worst 45 min. (The mean time between deep fades was about 10 s.) The frequent fades during the past solar maximum were also reported by El-Arini based on a campaign at Naha, Japan. The Japan data contain 9 s median time between fades (and 40 s mean time between fades) at 25 dB fading during 20:30 - 23:00 (local time) on 20 March 2002 (El-Arini, personal communication, April 22, 2009). If less frequent fades are included in the analysis, the distribution in Fig. 5 would have a fatter tail, and the distribution may not be well modeled by an exponential distribution. However, an empirical PDF with a thinner tail than the actual distribution, in this case, can provide a conservative representation of the statistics of the time between deep fades for our availability analysis. Hence, the actual distribution can still be conservatively modeled by an exponential distribution with a thinner tail. In order to provide a conservative model for our availability study in Section 5, we selected the worst 45 min data with the most frequent deep fades. In addition, we discarded sample points with more than 100 s time between deep fades for obtaining the empirical PDF. Note that the empirical PDF in Fig. 5 does not represent a nominally observed scintillation of solar maxima. It represents very frequent deep fades which have not been

usually observed even during solar maxima. The authors are not aware of an observed situation with more frequent deep fades under scintillation than Fig. 5.

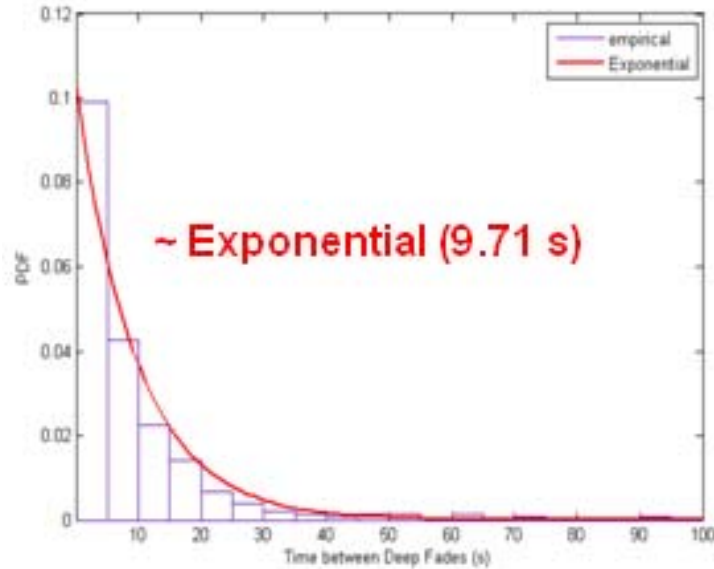


Fig. 5. Empirical probability density function of time between deep fades during the worst 45 min scintillation at Ascension Island. The time between deep fades approximately follows the exponential distribution with a mean of 9.71 s.

An important implication of the exponentially-distributed time between deep fades is that the corresponding counting process of number of deep fades is a Poisson process (Gallager, 1995). Fig. 6 illustrates this relationship. The time between deep fades corresponds to an inter-arrival time of a generic arrival process. Since the inter-arrival time (or the time between deep fades) follows the exponential distribution with a mean of 9.71 s, the counting process of the number of arrivals (or the number of deep fades) is the Poisson process of rate $\frac{1}{9.71 \text{ s}}$. The counting process, $\{N(t), t \geq 0\}$, can have zero and positive integer values for each nonnegative real number t .

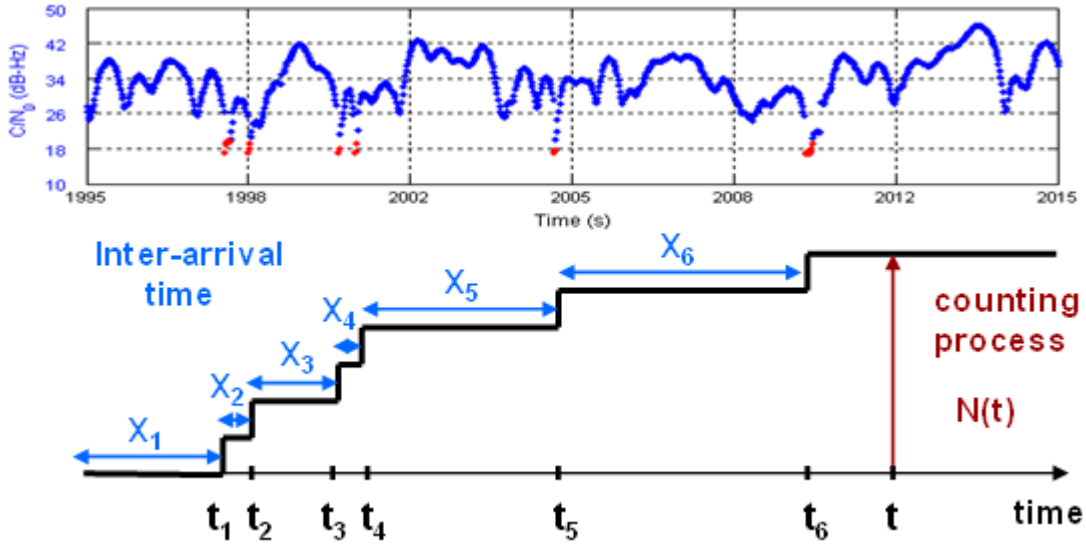


Fig. 6. Modeling a fading process (a counting process of the number of deep fades) as a Poisson process. The inter-arrival time (time between deep fades), X_i , follows an exponential distribution if, and only if, the counting process of the number of arrivals (number of deep fades), $\{N(t), t \geq 0\}$, is a Poisson process. The arrival times, t_i , represent the instances of deep fades indicated in red on the top plot.

The Poisson process has many interesting properties. For instance, if the $\{N(t), t \geq 0\}$ of Fig. 6 is a Poisson process of rate λ , the $N(t)$ for a given time t is a Poisson random variable with a mean and variance λt . If two independent Poisson processes of rates λ_1 and λ_2 are combined together, the resulting process is still a Poisson process of added rate $\lambda_1 + \lambda_2$ (Gallager, 1995). Using this property, we can generate two correlated Poisson processes from three independent Poisson processes (Fig. 7).

In Fig. 7, the common Poisson process of rate λ (the red Poisson process) is combined with two independent Poisson processes of rates $\lambda_1 - \lambda$ and $\lambda_2 - \lambda$. The result is two correlated Poisson processes of rates λ_1 and λ_2 . Let the common Poisson process be $\{C(t), t \geq 0\}$ and the two correlated Poisson processes be $\{V_1(t), t \geq 0\}$ and $\{V_2(t), t \geq 0\}$. Since the covariance between $V_1(t)$ and $V_2(t)$ for a given t is the same as the variance of $C(t)$ for the given t (see the Appendix for proof), the correlation coefficient between $V_1(t)$ and $V_2(t)$ for the given t is obtained as Eq. (5). Note that $C(t)$, $V_1(t)$, and $V_2(t)$ for a given

t are Poisson random variables with means and variances of λt , $\lambda_1 t$, and $\lambda_2 t$, respectively, because $\{C(t), t \geq 0\}$, $\{V_1(t), t \geq 0\}$, and $\{V_2(t), t \geq 0\}$ are Poisson processes of rates λ , λ_1 , and λ_2 , respectively.

$$\begin{aligned} \rho &= \frac{\text{Cov}[V_1(t), V_2(t)]}{\sqrt{\text{Var}[V_1(t)]}\sqrt{\text{Var}[V_2(t)]}} = \frac{\text{Var}[C(t)]}{\sqrt{\text{Var}[V_1(t)]}\sqrt{\text{Var}[V_2(t)]}} \\ &= \frac{\lambda t}{\sqrt{\lambda_1 t}\sqrt{\lambda_2 t}} = \frac{\lambda}{\sqrt{\lambda_1}\sqrt{\lambda_2}} \end{aligned} \quad (5)$$

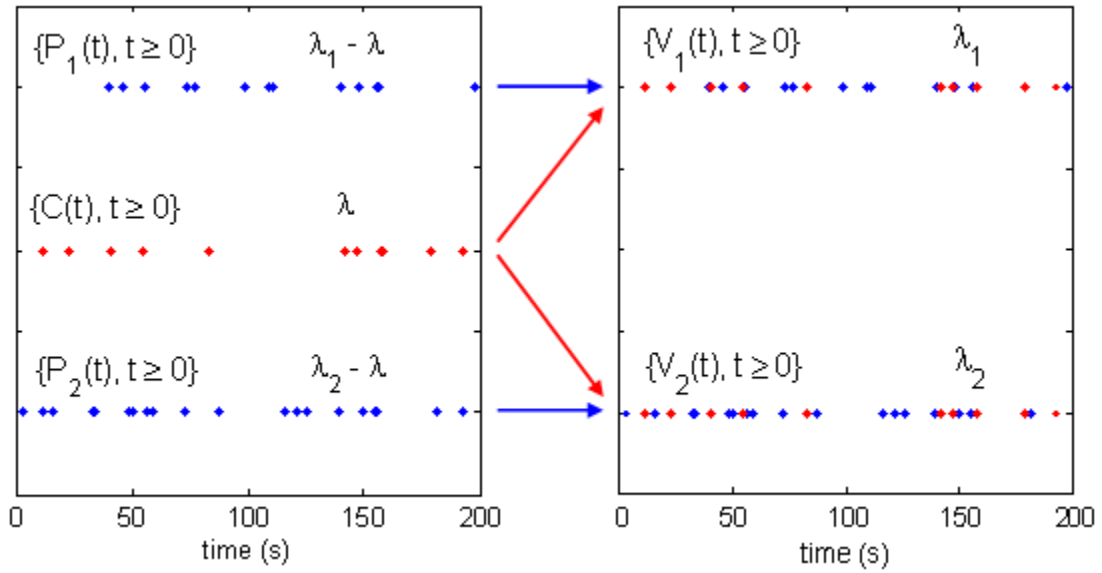


Fig. 7. Generation of two correlated Poisson processes of rates λ_1 and λ_2 from three independent Poisson processes of rates $\lambda_1 - \lambda$, λ , and $\lambda_2 - \lambda$. A common Poisson process of rate λ (the red Poisson process in the middle) is combined with two independent Poisson processes of rates $\lambda_1 - \lambda$ and $\lambda_2 - \lambda$ to generate two correlated Poisson processes of rates λ_1 and λ_2 .

The physical interpretation of λt is the expected number of arrivals of a Poisson process of rate λ during an interval t . Hence, if a fading process is modeled as a Poisson process of rate λ , for example, λt is interpreted as the expected number of deep fades during an interval t . The common Poisson process, $\{C(t), t \geq 0\}$, in Fig. 7 models the instances of simultaneous deep fades between two satellite channels. The correlated Poisson processes, $\{V_1(t), t \geq 0\}$ and $\{V_2(t), t \geq 0\}$, model the instances of the correlated deep

fades of the satellite 1 and satellite 2 channels, respectively. Therefore, the correlation coefficient of Eq. (5) can be interpreted as follows, if correlated fading processes are modeled as correlated Poisson processes.

$$\rho = \frac{\lambda t}{\sqrt{\lambda_1 t} \sqrt{\lambda_2 t}} = \frac{\text{Expected number of simultaneous deep fades during } t}{\sqrt{\text{Expected number of deep fades of satellite 1 during } t} \sqrt{\text{Expected number of deep fades of satellite 2 during } t}} \quad (6)$$

This correlation coefficient exactly describes how often satellite 1 and satellite 2 channels experience deep fades simultaneously; hence, this is a proper metric to measure the probability of simultaneous deep fades between two channels.

Once the time series of the signal intensity of two satellite channels are given, the “sample” correlation coefficient, $\hat{\rho}$, of deep fades during an observation time window T can be estimated using Eq. (7).

$$\hat{\rho}(T) = \frac{\text{Number of simultaneous deep fades between satellite 1 and 2}}{\sqrt{\text{Number of deep fades of satellite 1}} \sqrt{\text{Number of deep fades of satellite 2}}} \quad (7)$$

Once the lock status of two satellite channels of a receiver during an observation time window T is given, the sample correlation coefficient of loss of lock can be similarly estimated by Eq. (8).

$$\hat{\rho}(T) = \frac{\text{Number of overlapping losses of lock between satellite 1 and 2}}{\sqrt{\text{Number of losses of lock of satellite 1}} \sqrt{\text{Number of losses of lock of satellite 2}}} \quad (8)$$

Note that Eq. (7) and (8) are the same as Eq. (3) and (4), respectively, which were used to study the satellite-to-satellite correlation based on the real scintillation data in Section 3. Therefore, the definition of the sample correlation coefficient in Section 3 is mathematically justified in this section. This definition of a correlation coefficient is mathematically derived from the statistical observation and makes good physical sense.

Furthermore, Fig. 7 illustrates a way to generate two correlated fading processes with an arbitrary correlation coefficient. The rate of deep fades (the number of deep fades of a

satellite channel per unit time) is known from the worst 45 min data (i.e., $\lambda_1 = \lambda_2 = \frac{1}{9.71}$).

Hence, we can obtain λ for an arbitrary correlation coefficient ρ from Eq. (5).

$$\lambda = \rho\sqrt{\lambda_1}\sqrt{\lambda_2} = \frac{\rho}{9.71} \quad (9)$$

Once λ is obtained for a given correlation coefficient, ρ , three independent Poisson processes, $\{P_1(t), t \geq 0\}$, $\{C(t), t \geq 0\}$, and $\{P_2(t), t \geq 0\}$, in Fig. 7 of rates $\lambda_1 - \lambda$, λ , and $\lambda_2 - \lambda$, respectively, can be generated. Finally, the correlated fading processes, $\{V_1(t), t \geq 0\}$ and $\{V_2(t), t \geq 0\}$, of rates λ_1 and λ_2 , respectively, with the correlation coefficient ρ are obtained by combining these three Poisson processes (Fig. 7).

5. Availability analysis of LPV-200 under severe scintillation scenarios

Now we have a method to generate fading channels with any fading rates and correlation coefficients. Fig. 8 illustrates our procedure to analyze the availability of LPV-200 under severe scintillation scenarios. GPS avionics calculate the confidence bound of its position solution at each epoch based on several parameters which are satellite clock and ephemeris error, code noise and multipath, troposphere error, and satellite geometry. This confidence bound, usually called “protection level”, ensures that the true position is within this bound with very high probability (99.99999%) for LPV-200. If vertical and horizontal protection levels are smaller than the vertical and horizontal alert limits of LPV-200 (35 m and 40 m, respectively), LPV-200 service is “available” for this epoch. If protection levels are greater than the alert limits, in other words, if the true position is not protected within a small-enough bound with very high confidence, GPS avionics must raise a flag and LPV-200 service must not be available for the epoch in order to guarantee navigation safety (usually called “integrity”).

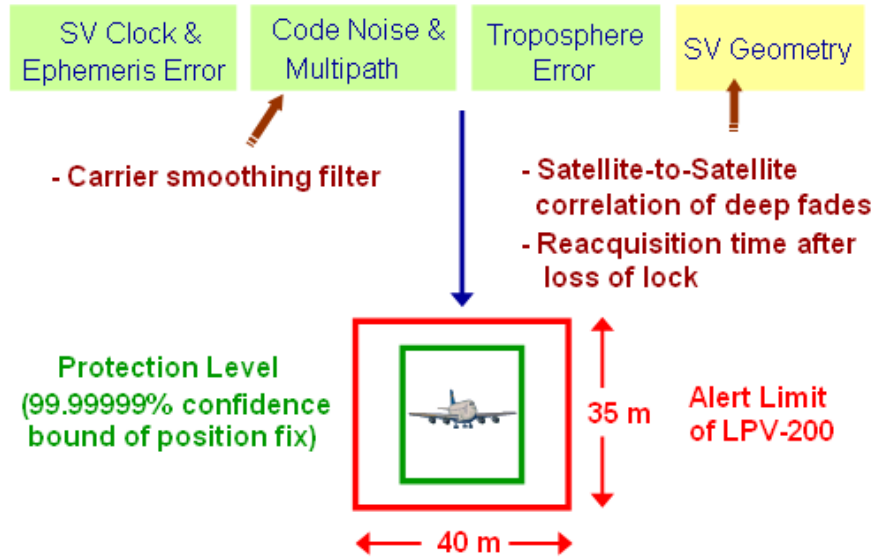


Fig. 8. Procedure to simulate the availability of LPV-200 under severe scintillation scenarios. The satellite geometry is impacted by the loss of lock after deep fading. (The instances of loss of lock are modeled by correlated Poisson processes considering satellite-to-satellite correlation of deep fades. The duration of loss of lock is determined by a receiver’s reacquisition time.) Frequent loss of lock increases code noise and multipath level in pseudorange measurements. (A carrier smoothing filter model is used to consider this effect.)

Without compromising the integrity, ionospheric scintillation reduces the availability in two ways. Deep signal fades caused by scintillation can break a receiver’s carrier tracking lock. Since the lost satellite channels cannot be used for position calculation, satellite geometry (the number and the distribution of satellites in view) is impacted during outage periods. Ideally, a GPS aviation receiver should maintain its carrier tracking lock for couple of hundred seconds to reduce the noise level of pseudorange measurements to the floor level by a carrier smoothing filter. Frequent loss of lock reduces effective lock time and increases the noise level of pseudorange measurements (Seo et al., 2009). The satellite loss and the increased noise level due to scintillation can increase protection levels over alert limits and consequently reduce navigation availability.

We modified the Matlab Algorithm Availability Simulation Tool (MAAST) (Jan et al., 2009) to incorporate scintillation effects such as the loss of lock after deep fades and the

shortened carrier smoothing time of a smoothing filter. For satellite clock and ephemeris errors, 1 m User Range Accuracy (URA) is assumed. The troposphere error model is from the WAAS MOPS. For the purpose of comparison, the satellite geometries are assumed to be the same as the satellite constellation of the observed worst-case scintillation period from the campaign at Ascension Island in 2001. Although we used the iono-free dual frequency code noise and multipath model for this analysis, the possible availability benefit depending on the correlation level between L1 and L5 deep fades was not taken into consideration. We assumed 100% correlation of deep fades between L1 and L5 channels. In other words, a receiver is assumed to lose its L5 channel as well whenever it loses its L1 channel after deep fading. Since the correlation level of deep fades between L1 and L5 frequencies is not yet known from real data, we take this most conservative approach in this paper. (As of April 2010, only one GPS satellite broadcasts an L5 test signal (Gao et al., 2009; Gunawardena et al., 2009) and there is no GPS L5 strong scintillation data available.)

The operational availabilities of LPV-200 under 45 min severe scintillation scenarios are presented in Fig. 9 with two parameters which are the correlation coefficient between two satellite channels and the reacquisition time of a receiver. Under the severe scintillation scenarios, all eight satellite channels are assumed to be affected by the very frequent deep fades observed in Ascension Island for the whole 45 min period. (In the real data, seven satellites were affected only during portions of the 45 min.) Even further, the deep fades of all satellite pairs are assumed to be correlated for the whole 45 min. (In the real data, the most correlated satellite pair experienced simultaneous deep fades with the correlation coefficient of 0.15 for the worst 300 s only.) Although adjacent satellites are more likely to be lost simultaneously under scintillation, the simultaneously lost satellite pairs (i.e., 4 pairs from the 8 satellites in view) in our analysis are selected in a way to maximize their separations. Since the simultaneous loss of distant satellites reduces the availability more than the simultaneous loss of adjacent satellites, our assumption is more conservative than a physically expected situation.

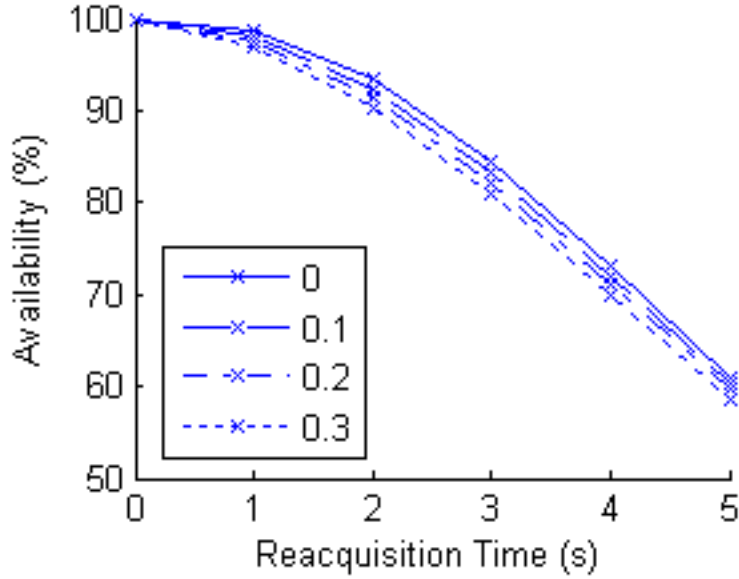


Fig. 9. Availability of LPV-200 under severe scintillation scenarios with various satellite-to-satellite correlation coefficients of deep fades (0, 0.1, 0.2, and 0.3). The availability result is more sensitive to a receiver’s reacquisition time than the correlation level. A 1 s reacquisition time provides more than 95% availability in these correlation levels.

After generating correlated fading processes with a correlation coefficient (every 0.1 from 0 to 0.3) by the method proposed in Section 4, a receiver’s reacquisition time (every 1 s from 0 to 5 s) was applied for the availability calculation. The operational availabilities of LPV-200 obtained under the severe scintillation scenarios are plotted in Fig. 9 with respect to these two parameters which are the correlation coefficient and the reacquisition time. Although the maximum observed correlation coefficient of deep fades in the Ascension Island data was 0.15, we considered four different correlation coefficients (0, 0.1, 0.2, and 0.3) for sensitivity study. As shown in Fig. 9, the satellite-to-satellite correlation of deep fades has less impact on the availabilities than the reacquisition time of a receiver. With a 1 s reacquisition time, we can expect more than 95% availability even under our severe scintillation scenarios with a correlation coefficient of 0.3.

It should be emphasized that the severe scintillation scenarios generated in this paper represent much worse cases than any observation in the literature including the Ascension

Island data itself. In our scenarios, every satellite channel always experiences very frequent deep fades, and four satellite pairs are always lost simultaneously with a given correlation coefficient. In addition, 100 % probability of loss of lock under deep fades is assumed. In other words, a receiver is assumed to lose its carrier tracking lock at every single deep fade with a 100 % probability. Further, a receiver is assumed to lose its L5 channel whenever it loses its L1 channel (100% correlation between L1 and L5 channel). Even with the severe scintillation scenarios and the conservative steps throughout our analysis, the result shows that a 1 s reacquisition time can provide more than 95% availability of LPV-200. Therefore, a fast reacquisition after a brief outage can be a very effective strategy to provide higher navigation availability under the given geometric diversity of satellites and the observed low satellite-to-satellite correlation of deep fades. As the certified aviation receiver during the Brazil campaign already demonstrated fast reacquisition (within 2 s in 91% cases), the one or two second reacquisition time after brief outages is technically attainable. The current MOPS does not have any performance requirement under scintillation (RTCA, 2006). Under the current MOPS, a generic certified aviation receiver can perform extensive safety check up to 20 s in principle before reintroducing the lost channel into position solutions depending on its algorithm, which can lead to severe availability loss under strong scintillation. This possibility should be discouraged by mandating a fast reacquisition after a very brief outage.

This paper focuses on the effect of amplitude fading due to scintillation and does not explicitly consider phase jitter which has been emphasized in (Kintner et al., 2009; Humphreys et al., 2009). The amount of phase jitter affects the probability of loss of lock in the 28-30 dB-Hz threshold range of the aviation receiver in the given data sets. This paper conservatively assumes that the receiver loses lock at 30 dB-Hz with 100% probability. Although losses of lock above 30dB-Hz are rare in the data sets for this research, strong phase scintillation can cause losses of lock at even higher C/N_0 especially in the auroral regions and the poles. Note that the fading process model of this paper generates instances of loss of lock based on the observations without considering the causes of loss of lock. Hence, the availability result of this section is conservatively valid regardless of the causes of loss of lock (deep amplitude fading and/or phase jitter) if

the instances of loss of lock of an aviation receiver are less frequent than the severe scintillation scenarios generated in this section. If more frequent losses of lock of an aviation receiver due to strong phase scintillation on top of strong amplitude scintillation are observed in the future, the availability analysis of this paper should be performed again with the same method but different parameters.

Another point to mention is that the scintillation data for this research were collected by stationary receivers. If the velocity of the ionospheric pierce point of a particular satellite channel and the velocity of electron density irregularities are closely matched each other due to dynamic motions of a plane, an aviation receiver onboard can experience a longer duration of fading for the corresponding satellite channel (Kintner et al., 2004). Similarly, if the velocity of an ionospheric pierce point and the velocity of irregularities are opposite to each other (i.e., velocity mismatch), the corresponding satellite channel can experience a shorter duration of fading. Due to the geometric diversity of GPS satellites, the velocities of ionospheric pierce points of different satellite channels are different to each other at any given epoch. Hence, if a certain satellite channel experiences longer fading at a given epoch due to the velocity match, the other satellite channels could experience shorter fading due to the velocity mismatch. A longer fading of a particular satellite channel due to the velocity match can increase the probability of simultaneous loss of lock on two or more satellites. It is unknown at this time if this effect is significant compared to the many other conservative measures implemented in our analysis. The effects of the velocity match or mismatch due to motions of a plane and electron density irregularities are not considered in this paper. However, the effects of platform motions on the GPS aviation availability under scintillation should be more carefully studied in future research.

Note that the correlated fading process model proposed in this paper is based on the limited observations during the past solar maximum. Hence, we introduced many conservative steps throughout the analysis because the observations may not represent the worst possible scintillation. The development of a more sophisticated scintillation model based on the physics of scintillation will better describe the signal environment, which

will enable a reduction of the conservative steps in this paper and predict the availability more precisely.

6. Conclusion

The correlation of signal fades between satellite channels must be studied to assess the operational availability of GPS aviation under strong ionospheric scintillation. Although a few researchers have tried to investigate the correlation between fading channels, an appropriate metric to measure the correlation level for GPS aviation applications has not been previously applied. This paper proposes a better definition of correlation coefficient, which describes the probability of simultaneous deep fades (and the probability of overlapping loss of lock) between channels.

Using our correlation metric, the satellite-to-satellite correlation was evaluated based on real scintillation data from the past solar maximum (the worst 45 min data from the nine day campaign at Ascension Island). The result quantitatively confirms that the correlation of deep fades between two satellite channels was very low (less than 15% correlation) even during the worst-case scintillation of the campaign at Ascension Island. It was also observed that the correlation between closely-spaced satellites was low as well during the Brazil campaign. Hence, notable availability benefit from the geometric diversity of satellites is attainable during strong scintillation. If a future GNSS receiver tracks both GPS and Galileo (the European GNSS under development), the number of satellites in view would be approximately doubled. Considering the low satellite-to-satellite correlation, this improved geometry from dual constellations will further increase the navigation availability significantly.

Although the signal environment under scintillation demonstrated low satellite-to-satellite correlation of deep fades, we have shown that the effective correlation experienced by a receiver (i.e., the correlation of loss of lock) can be much higher depending on a receiver's reacquisition capability. Using the correlated fading process model proposed

in this paper, the availabilities of LPV-200 under severe scintillation scenarios are analyzed with the consideration of a receiver's reacquisition times. The result confirms that the reacquisition time is the most sensitive parameter for the availability under the given satellite geometry. Therefore, a fast reacquisition after a brief outage, which has been already demonstrated by a certain model of a certified aviation receiver, should be mandated in the future WAAS MOPS to guarantee much higher availability under scintillation (more than 95% availability of LPV-200 under severe scintillation scenarios). Without this requirement, a generic aviation receiver may provide less than 50% availability of LPV-200 during severe scintillation.

Acknowledgement

The authors gratefully acknowledge the Federal Aviation Administration (FAA) CRDA 08-G-007 for supporting this research and Theodore Beach, AFRL, and Eurico de Paula, INPE, Brazil, for providing the data sets. The authors also appreciate the valuable comments from Seebany Datta-Barua, San Jose State University. The opinions discussed here are those of the authors and do not necessarily represent those of the FAA or other affiliated agencies.

References

- Aarons, J. Global morphology of ionospheric scintillations. *Proceedings of the IEEE*, 70(4), 360–378, 1982.
- Cabler, H., DeCleene, B. LPV: New, improved WAAS instrument approach. In: *Proceedings of 15th International Technical Meeting*, Portland, OR, September 24-27, 2002 (available www.ion.org).
- Conker, R. S., El-Arini, M. B., Hegarty, C. J., Hsiao, T. Modeling the effects of ionospheric scintillation on GPS/Satellite-Based Augmentation System availability. *Radio Sci.*, 38(1), 1001, doi:10.1029/2000RS002604, 2003.

Crane, R. K. Ionospheric scintillation. *Proc. IEEE*, 65, 180–199, doi:10.1109/PROC.1977.10456, 1977.

Datta-Barua, S., Walter, T., Blanch, J., Enge, P. Bounding higher-order ionosphere errors for the dual-frequency GPS user. *Radio Sci.*, 43, RS5010, doi:10.1029/2007RS003772, 2008.

El-Arini, M. B., Conker, R. S., Ericson, S. D., Bean, K. W., Niles, F., Matsunaga, K., Hoshinoo, K. Analysis of the effects of ionospheric scintillation on GPS L2 in Japan. In: *Proceedings of 16th International Technical Meeting*, Portland, OR, September 9-12, 2003 (available www.ion.org).

Enge, P., Walter, T., Pullen, S., Kee, C., Chao, Y.-C., Tsai, Y.-J. Wide area augmentation of the global positioning system. *Proc. IEEE*, 84, 1063–1088, doi:10.1109/5.533954, 1996.

Gallager, R. G. *Discrete stochastic processes*, Kluwer Academic Publishers, 1995.

Gao, G. X., Heng, L., De Lorenzo, D., Lo, S., Akos, D., Chen, A., Walter, T., Enge, P., Parkinson, B. Modernization milestone: observing the first GPS satellite with an L5 payload. *Inside GNSS*, May/June, 30-36, 2009 (available www.insidegnss.com).

Gunawardena S., Zhu, Z., Braasch, M. First look: observing the GPS L5 test transmission from SVN49 using software radio processing. *Inside GNSS*, May/June, 22-29, 2009 (available www.insidegnss.com).

Gwal A. K., Dubey, S., Wahi, R. A study of L-band scintillations at equatorial latitudes. *Advances in Space Research*, 34, 2092-2095, doi:10.1016/j.asr.2004.08.005, 2004.

Hegarty, C. J., Chatre, E. Evolution of the Global Navigation Satellite System (GNSS). Proc. IEEE, 96, 1902-1917, doi:10.1109/JPROC.2008.2006090, 2008.

Humphreys, T. E., Psiaki, M. L., Hinks, J. C., O'Hanlon, B., Kintner, P. M. Simulating ionosphere-induced scintillation for testing GPS receiver phase tracking loops. IEEE Journal of Selected Topics in Signal Processing, 3, 707-715, doi: 10.1109/JSTSP.2009.2024130, 2009.

Jan, S.-S., Chan, W., Walter, T. MATLAB algorithm availability simulation tool. GPS Solutions, 13, 327-332, doi:10.1007/s10291-009-0117-4, 2009.

Jin, S., Luo, O. F., Park P. GPS observations of the ionospheric F2-layer behavior during the 20th November 2003 geomagnetic storm over South Korea. Journal of Geodesy, 82(12), 883-892, doi:10.1007/s00190-008-0217-x, 2008.

Kaplan, E., Hegarty, C., Eds. Understanding GPS: Principles and Applications, 2nd ed. Norwood, MA: Artech House, 2006.

Kintner, P. M., Ledvina, B. M., de Paula, E. R., Kantor, I. J. Size, shape, orientation, speed, and duration of GPS equatorial anomaly scintillations. Radio Sci., 39, RS2012, doi:10.1029/2003RS002878, 2004.

Kintner, P., Humphreys, T., Hinks, J. GNSS and ionospheric scintillation: how to survive the next solar maximum. Inside GNSS, July/August, 22-30, 2009 (available www.insidegnss.com).

May, M., Brown, A., Tanju, B. Applications of digital storage receivers for enhanced signal processing. In: Proceedings of 12th International Technical Meeting, Nashville, TN, September 14-17, 1999 (available www.ion.org).

Misra, P., Enge, P. Global Positioning System: Signals, Measurements, and Performance, 2nd ed. Lincoln, MA: Ganga-Jamuna, 2006.

Normark, P.-L., Stahlberg, C. Hybrid GPS/Galileo real time software receiver. In: Proceedings of 18th International Technical Meeting, Long Beach, CA, September 13-16, 2005 (available www.ion.org).

Parkinson B. W. Origins, evolution, and future of satellite navigation. *Journal of guidance, control, and dynamics*, 20, 11-25, 1997.

Radio Technical Commission for Aeronautics (RTCA). Minimum operational performance standards for global positioning system/wide area augmentation system airborne equipment, Doc. DO-229D, Washington, D. C., 2006.

Rama Rao, P. V. S., Gopi Krishna, S., Niranjana, K., Prasad, D. S. V. V. D. Study of spatial and temporal characteristics of L-band scintillations over the Indian low-latitude region and their possible effects on GPS navigation, *Ann. Geophys.*, 24, 1567-1580, 2006.

Seo, J., Walter, T., Chiou, T.-Y., Enge, P. Characteristics of deep GPS signal fading due to ionospheric scintillation for aviation receiver design. *Radio Sci.*, 44, RS0A16, doi:10.1029/2008RS004077, 2009.

Seo, J., Walter, T., Enge, P. Availability impact on GPS aviation due to strong ionospheric scintillation. Accepted for publication in *IEEE Transactions on Aerospace and Electronic Systems*, 2010.

Walter, T., Enge, P., Blanch, J., Pervan, B. Worldwide vertical guidance of aircraft based on modernized GPS and new integrity augmentations. *Proc. IEEE*, 96, 1918-1935, doi:10.1109/JPROC.2008.2006099, 2008.

Appendix

This appendix proves $\text{Cov}[V_1(t), V_2(t)] = \text{Var}[C(t)]$ for a given t , where $V_1(t)$, $V_2(t)$, and $C(t)$ are given as in Fig. 7.

Since the Poisson random variables, $P_1(t)$, $P_2(t)$, and $C(t)$, in Fig. 7 for a given t are all independent,

$$\begin{aligned} E[V_1(t) V_2(t)] &= E[\{P_1(t) + C(t)\} \{P_2(t) + C(t)\}] \\ &= E[P_1(t)P_2(t) + P_1(t)C(t) + P_2(t)C(t) + C(t)^2] \\ &= E[P_1(t)] E[P_2(t)] + E[P_1(t)] E[C(t)] + E[P_2(t)] E[C(t)] + E[C(t)^2] \end{aligned}$$

$$\begin{aligned} E[V_1(t)] E[V_2(t)] &= E[P_1(t) + C(t)] E[P_2(t) + C(t)] \\ &= \{E[P_1(t)] + E[C(t)]\} \{E[P_2(t)] + E[C(t)]\} \\ &= E[P_1(t)] E[P_2(t)] + E[P_1(t)] E[C(t)] + E[P_2(t)] E[C(t)] + E[C(t)]^2. \end{aligned}$$

Hence,

$$\begin{aligned} \text{Cov}[V_1(t), V_2(t)] &= E[V_1(t) V_2(t)] - E[V_1(t)] E[V_2(t)] \\ &= E[C(t)^2] - E[C(t)]^2 \\ &= \text{Var}[C(t)]. \end{aligned}$$